CURVE SEGMENTATION USING DIRECTIONAL INFORMATION, RELATION TO PATTERN DETECTION

Eric Pichon, Allen Tannenbaum

Georgia Institute of Technology
{eric, tannenba}@ece.gatech.edu

ABSTRACT

We propose an extension of the conformal (or geodesic) active contour framework in which the conformal factor depends not only on the position of the curve but also on the direction of its tangent. We describe several properties for variational curve segmentation schemes that justify the construction of optimal conformal factors (i.e., learning) in strong connection with pattern matching. The determination of optimal curves (i.e., segmentation), can be performed using either the calculus of variations or dynamic programming. The technique is illustrated on a road detection problem for different signal to noise ratios.

1 Introduction

Image segmentation, which we will define here as the determination of structures in an image, is a central problem of artificial vision. Elongated structures such as roads in a 2D aerial photography or an arteries in a 3D computed tomography dataset can be represented by open curves. Closed planar curves can be used to delimit regions in 2D. In this work we will consider the general problem of detecting open or closed curves Γ from n-dimensional images I on some p-dimensional color space.

$$\Gamma : [0,1] \to \mathbb{R}^n \text{ and } I : \mathbb{R}^n \to \mathbb{R}^p \tag{1}$$

Kass *et al.* introduced the *snake* or *active contour* model [5] in which an initial curve $\Gamma_{|t=0}$ is deformed in order to minimize an energy $E(\Gamma, I)$. This framework was given a differential-geometric interpretation and implemented via level sets in [2, 6]. In [2] this is called *geodesic active contours* and in [6] the model is referred to as *conformal active contours*. Since the flow in both papers is not really an intrinsic geodesic minimizing flow, we prefer the term "conformal" which we will use throughout this paper. The underlying energy functional in the model is

$$E(\Gamma, \Psi_I) \triangleq \int_\Gamma \Psi_I(\Gamma(s))\, \mathrm{d}s, \tag{2}$$

where the conformal factor

$$\Psi_I : \mathbb{R}^n \to \mathbb{R}^+ \tag{3}$$

is constructed from the image, for example by taking some decreasing function of some edge detector. A standard choice for scalar images is $\Psi_I(\boldsymbol{x}) = 1/(1 + \|\nabla I(\boldsymbol{x})\|)$.

Since Ψ is small near edges, edges will attract the curve Γ as it is deformed to minimize the energy (2). Moreover since (2) is the Ψ-weighted length, any irregularities of Γ will be penalized.

A number of different approaches using more global constraints have also been proposed such as in [8, 16]; see the book [11] and references therein.

While the conformal active contour formulation is very elegant (in particular it is variational and has a geometric interpretation) it does not ensure that the curve be *aligned* with the boundary. In fact direction information is completely absent and the formulation is purely isotropic. In this work we propose to introduce directional information according to

$$E(\Gamma, \Psi_I) \triangleq \int_\Gamma \Psi_I(\Gamma(s), \Gamma_s(s))\, \mathrm{d}s, \tag{4}$$

where the conformal factor Ψ_I is not only a function of the location of the position of the curve but also its tangent direction Γ_s on the unit sphere $\mathbb{S}^{n-1}$.

$$\Psi_I : \mathbb{R}^n \times \mathbb{S}^{n-1} \to \mathbb{R}^+ \tag{5}$$

In this framework, a cost is attributed at each point to each direction of space. This is more general than previous extensions of the conformal active contour model proposed independently in [15, 7, 10] where direction information is reduced to a vector field $\boldsymbol{v}$ and the conformal factor is of the form $\Psi_I(\boldsymbol{x}, \overrightarrow{d}) = \overrightarrow{d}.\boldsymbol{v}(\boldsymbol{x})$.

We propose in Section 2 a set of natural properties which indicates the strong ties between our approach and pattern matching. We then propose a parametric pattern matching model and show how optimal (according to our functional) conformal factors can be determined. In Section 3 we show how optimal curves can be determined (i.e., how to segment the image) using the calculus of variations or dynamic programming. Examples of this directional segmentation of real images are shown in Section 4. Due to space constraints full mathematical will be provided in [9].

This work was partly supported by NIH through NAC and NAMIC (Brigham and Women's Hospital)

2 Pattern Detection

We would like to construct conformal factors from some local pattern detector. We will show how this can be motivated by a several natural properties which we want our scheme to satisfy, and then propose a particular pattern detector inspired by image matching.

2.1 Properties of Conformal Factor

Here, $\xrightarrow{c}$ denotes convergence with respect to some chosen norm.

- Continuity with respect to the curve
$$(\Gamma' \xrightarrow{c} \Gamma) \Rightarrow (E(\Gamma', \Psi_I) \xrightarrow{c} E(\Gamma, \Psi_I)) \quad \text{(P1)}$$
Human experts typically do not agree perfectly on the position of a certain feature. It is important to capture the inherently fuzzy nature of segmentation.

- Continuity with respect to the image
$$(I' \xrightarrow{c} I) \Rightarrow (E(\Gamma, \Psi_{I'}) \xrightarrow{c} E(\Gamma, \Psi_I)) \quad \text{(P2)}$$
The presence of (limited) noise on the image should not impact drastically the segmentation result.

- Locality of information employed
$$\exists r_0 > 0, \forall \Gamma, \forall I, I', \\ (\forall \boldsymbol{x} \in \mathbb{R}^n, d(\boldsymbol{x}, \Gamma) < r_0 \Rightarrow (I(\boldsymbol{x}) = I'(\boldsymbol{x})) \\ \Rightarrow (E(\Gamma, \Psi_{I'}) = E(\Gamma, \Psi_I)) \quad \text{(P3)}$$
Only information near the curve should be used[1].

- Invariance with respect to Euclidean transformations[2]
$$\forall T \text{ Euclidean mapping } \mathbb{R}^n \to \mathbb{R}^n, \\ E(\Gamma, \Psi_{I \circ T}) = E(T \circ \Gamma, \Psi_I) \quad \text{(P4)}$$
The image is not assumed to be oriented in a meaningful way.

2.2 Pattern Detector

It can be shown [9] that the conformal factors that respect (P4) are of the form:
$$\Psi(\boldsymbol{x}, \overrightarrow{d}) = \Phi(I \circ T_{\mathbf{0}, \overrightarrow{e_1} \to \boldsymbol{x}, \overrightarrow{d}}) \quad (6)$$
where $T_{\mathbf{0}, \overrightarrow{e_1} \to \boldsymbol{x}, \overrightarrow{d}}$ is a Euclidean transformation that maps point $\mathbf{0}$ into point $\boldsymbol{x}$ and direction $\overrightarrow{e_1}$ into direction $\overrightarrow{d}$ and $\Phi : (\mathbb{R}^n \to \mathbb{R}^p) \to \mathbb{R}^+$ detects (i.e., is small for) patterns located at $\mathbf{0}$ (e..g the center of the image) and oriented along $\overrightarrow{e_1}$ (e.g., the first direction of the canonical basis). The transformation is defined uniquely up to a rotation around $\overrightarrow{e_1}$ and Φ has to be invariant with respect to such rotations.

[1] This is a bottom-up assumption. We exclude here higher forms of top-down reasoning, for example determining the location of an artery from that of the organs to which it is connected.

[2] By *Euclidean transformations* we mean the group of rigid transformations generated by rotations and translations.

The energy (4) can be rewritten
$$E(\Gamma, \Psi_I) = \int_\Gamma \Phi \circ I \circ T_\Gamma(s) \, \mathrm{d}s, \quad (7)$$
where $T_\Gamma(s) = T_{\mathbf{0}, \overrightarrow{e_1} \to \Gamma(s), \overrightarrow{\Gamma_s(s)}}$, i.e., $I \circ T_\Gamma(s)$ is a version of the image that has been centered at $\Gamma(s)$ and aligned with the local tangent $\Gamma_s(s)$.

We propose to use a parametric model for Φ. If the image is expressed in cylindrical coordinates $I(l, r, \boldsymbol{\theta})$ where l is the abscissa along the axis $\overrightarrow{e_1}$ we define
$$\Phi(I) \triangleq \int_l \int_r \int_{\boldsymbol{\theta}} [I(l, r, \boldsymbol{\theta}) - \mu(l, r)]^t \Sigma^{-1}(l, r) \\ [I(l, r, \boldsymbol{\theta}) - \mu(l, r)] \, \mathrm{d}^{n-2}\boldsymbol{\theta} \, r^{n-2} \, \mathrm{d}r \, \mathrm{d}l. \quad (8)$$
Note that as stated before, Φ is invariant with respect to rotations around $\overrightarrow{e_1}$. It can be interpreted as a Mahalanobis distance with a mean vector field $\mu : \mathbb{R}^2 \to \mathbb{R}^p$ and a positive semi-definite covariance matrix field $\Sigma : \mathbb{R}^2 \to S^+(\mathbb{R}^p)$. In order to satisfy the locality axiom (P3) we set $\Sigma^{-1}(l, r) = \mathbf{0}$ for l and r larger than some constant r_0. In order to satisfy the continuity properties, (P1) and (P2) both fields have to be continuous.

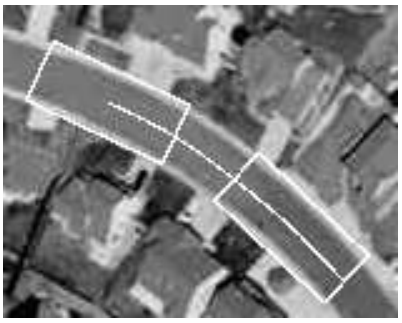

Fig. 1. The centerline (white curve) is determined manually. It is used to define pattern samples such as the two white boxes.

Given a sample image I for which some optimal curve Γ^* is given (for example by a human expert), we obtain a set of positive examples $\{ I_p^+ \}_{p=1 \ldots n^+}$ of the pattern under consideration by applying the aligning transforms $T_{\Gamma^*}(s)$ to I for different values of the arc-length parameter s. This is illustrated on Fig. 1. In this work we defined the fields $\Phi^* \triangleq (\mu^*, \Sigma^*)$ to be the mean and covariance of these positive examples. If the number of examples is large and they are uniformly sampled, we achieve a Monte-Carlo approximation and we can then show that if Ψ_I^* is constructed from Φ^* according to (6) then it is optimal in the sense that
$$\Psi_I^* = \arg\min_{\Psi_I} E(\Gamma^*, \Psi_I). \quad (9)$$

This procedure respects the additional property:

- Invariance with respect to invertible affine transformations of the color space

$$\forall \Gamma^*, I, T \text{ affine invertible } \mathbb{R}^p \to \mathbb{R}^p, \quad \Psi^*_{T\circ I} = \Psi^*_I \quad \text{(P5)}$$

3 Image Segmentation

Given a conformal factor Ψ_I (which can be obtained from an image I and a pattern detector Φ as described in Section 2), the segmentation problem is to determine optimal curves

$$\Gamma^* = \arg\min_{\Gamma\in\mathcal{G}} E(\Gamma, \Psi_I), \tag{10}$$

where $\mathcal{G}$ is the space of curves of interest. This could be for example the set of all closed curves or of open curves between two user-supplied points.

3.1 Calculus of Variations

As is standard, we can use the calculus of variations to compute the first variation from which we derive a gradient descent evolution. In the case of (4), the evolution equation derived in this matter is

$$\frac{\partial \Gamma}{\partial t} = -P_{(\Gamma_s)^\perp}(\nabla_1\Psi - \frac{\partial}{\partial s}\nabla_2\Psi) + \Psi\Gamma_{ss}, \tag{11}$$

where $P_{(\Gamma_s)^\perp}$ is the projection on the plane locally normal to the curve and $\nabla_1\Psi$ and $\nabla_2\Psi$ are the gradient of the conformal factor (5) with respect to location and direction respectively. This last terms constitutes the difference with the isotropic conformal active contour model [2, 6].

3.2 Dynamic Programming

Dynamic programming was initially proposed in the 50's by Bellman and his school [1] for optimal control. The fundamental idea is to choose a seed point $\boldsymbol{s}$ and to define the minimal energy for open curves of extremities $\boldsymbol{s}$ and $\boldsymbol{x}$, for all $\boldsymbol{x} \in \mathbb{R}^n$.

$$E^*(\boldsymbol{x}, \Psi) \triangleq \min_{\Gamma\in\mathcal{G}(\boldsymbol{s},\boldsymbol{x})} E(\Gamma, \Psi) \tag{12}$$

The value function E^* satisfies the Hamilton-Jacobi-Bellman equation

$$\begin{cases} 0 = \max\limits_{\overrightarrow{d}\in\mathbb{S}^{n-1}} \{ \nabla E^*(\boldsymbol{x}).\overrightarrow{d} - \Psi_I(\boldsymbol{x}, \overrightarrow{d}) \} & \forall \boldsymbol{x} \in \mathbb{R}^n \\ 0 = E^*(\boldsymbol{s}) \end{cases} \tag{13}$$

which can be solved numerically for E^* and $\overrightarrow{d^*}$ (the local maximal direction) using recently proposed iterative [4] or single-pass [13] algorithms.

For any point $\boldsymbol{x} \in \mathbb{R}^n$, the *globally* optimal curve $\Gamma^* = \arg\min_{\Gamma\in\mathcal{G}(\boldsymbol{s},\boldsymbol{x})} E(\Gamma, \Psi)$ back to $\boldsymbol{s}$ can be determined by following the vector field $\overrightarrow{d^*}$.

In the isotropic case, $\overrightarrow{d^*}$ is aligned with ∇E^*. Equation (13) reduces to the Eikonal equation $\|\nabla E^*(\boldsymbol{x})\| = \Psi_I(\boldsymbol{x})$ which can be solved using the Fast Marching method [14, 12] or approximated using Dijkstra's algorithm as in the LiveWire algorithm [3].

4 Results

The algorithm was applied to a road detection task. A small portion of the road was outlined manually (Fig. 1) to determine the pattern detector as described in Section 2.

(a) Calculus of variation. The initial curve is in white, final result in black. A few intermediate curves are shown in gray.

(b) Dynamic programing. The seed region is a disc at the crossroad (not represented).

Fig. 2. Examples of segmentation.

The two techniques (calculus of variations and dynamic programing) proposed in Section 3 result in correct segmentations (Fig. 2).

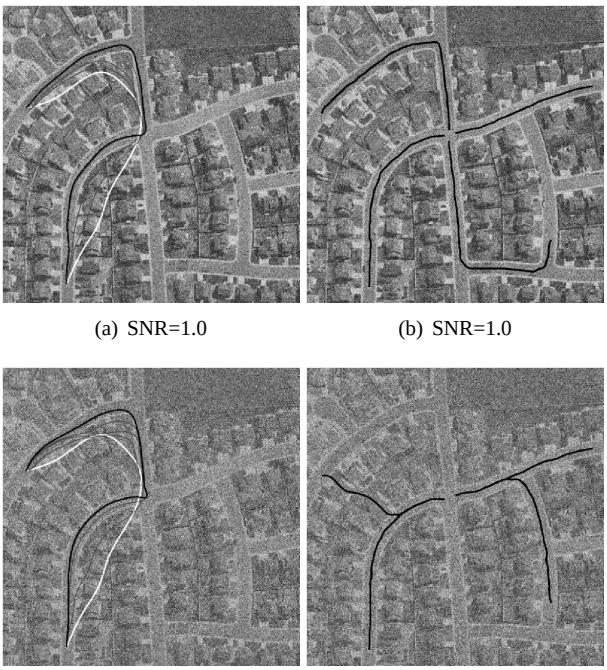

(a) SNR=1.0 (b) SNR=1.0

(c) SNR=0.5 (d) SNR=0.5

Fig. 3. Segmentations at different Signal to Noise ratios. Compare to Fig. 2.

As shown on Fig. 3, the algorithm is fairly resistant to noise[3]. Note that in the extreme case where the energy of the noise is the double of the energy of the image roads are still recovered mostly correctly by both approaches. It is interesting to notice that dynamic programing resulted in two different but equally valid ways to reach the crossroad from the bottom right of the image (Fig. 3(b) and 3(d)). An incorrect "shortcut" was found in Fig. 3(d) from the top left corner. Note that on the same region calculus of variation resulted in the correct segmentation (Fig. 3(c)). In that case, the correct (with respect to the road detection task) curve is not the global minimum of the energy (or else it would have been determined by dynamic programing). In that case, calculus of variations being essentially a gradient descent technique, converged to a local minimum closer to its starting point (the initial curve). The sensitivity to local minima is therefore sometimes desirable since it gives the user some control over the final segmentation.

5 Future Research

Future research will focus on the learning procedure as well as slightly modified versions of the functional (4).

[3]Gaussian white noise was added to the image.

The technique will be applied to the segmentation of medical images such as arteries from computed tomography datasets or neural tracts from diffusion weighted magnetic resonance imagery.

6 References

[1] R.E. Bellman. *Dynamic Programming*. Princeton University Press, Princeton, N.J, 1957.

[2] V. Caselles, R. Kimmel, and G. Sapiro. Geodesic active contours. *Int. Journal Computer Vision*, 22:61–79, 1997.

[3] A. Falcao, J. Udupa, S. Samarasekera, and S. Sharma. User-steered image segmentation paradigms: Livewire and live-lane. *Graphical Models and Image Processing*, 60(4):233–260, 1998.

[4] C.Y. Kao, S. Osher, and Y. Tsai. Fast sweeping methods for static Hamilton-Jacobi equations. Technical Report 03-75, UCLA CAM, December 2003. under review, SIAM Journal on Numerical Analysis.

[5] M. Kass, A. Witkin, and D. Terzopoulos. Snakes: active contour models. *Int. Journal of Computer Vision*, 1:321–331, 1987.

[6] S. Kichenassamy, A. Kumar, P. Olver, A. Tannenbaum, and A. Yezzi. Conformal curvature flows: from phase transitions to active contours. *Archive for Rational Mechanics and Analysis*, 134:275–301, 1996.

[7] R. Kimmel and A. M. Bruckstein. Regularized laplacian zero crossings as optimal edge integrators. *International Journal of Computer Vision*, 53(3):225 – 243, 2003.

[8] N. Paragios and R. Deriche. Geodesic active regions: A new framework to deal with frame partiton problems in computer vision. *Journal of Visual Communication and Image Representation*, 13:249–268, 2002.

[9] E. Pichon. *Pattern detection and image segmentation with anisotropic conformal factors*. PhD thesis, Georgia Institute of Technology, 2005. In preparation.

[10] E. Pichon, G. Sapiro, and A. Tannenbaum. *Segmentation of Diffusion Tensor Imagery*, volume 286 of *Directions in Mathematical Systems Theory and Optimization*, pages 239–247. Springer-Verlag Heidelberg, January 2003.

[11] G. Sapiro. *Geometric Partial Differential Equations and Image Analysis*. Cambridge University Press, 2001.

[12] J.A. Sethian. *LevelSet Methods and Fast Marching Methods*. Cambridge University Press, 1999.

[13] J.A. Sethian and A. Vladimirsky. Ordered upwind methods for static Hamilton-Jacobi equations: Theory and applications. *SIAM J. on Numerical Analysis*, 41(1):325–363, 2003.

[14] J. N. Tsitsiklis. Efficient algorithms for globally optimal trajectories. *IEEE Transactions on Automatic Control*, 50(9):1528–1538, 1995.

[15] A. Vasilevskiy and K. Siddiqi. Flux maximizing geometric flows. *IEEE Trans. Pattern Anal. Mach. Intell.*, 24(12):1565–1578, 2002.

[16] A. Yezzi, A. Tsai, and A. Willsky. A fully global approach to image segmentation via coupled curve evolution equations. *Journal of Visual Communication and Image Representation*, 13:195–216, 2002.